

# Study on Antibacterial Mechanism of Two-dimensional Nanomaterial $Ti_3C_2$ -Ag Complexes

Xiaobo Zhu, Shaolong Chen, Yongqiang Jiang\*

State Key Laboratory of Pathogen and Biosecurity, Beijing Institute of Microbiology and Epidemiology, Beijing 100071, China.

**How to cite this paper:** Xiaobo Zhu, Shaolong Chen, Yongqiang Jiang. (2022). Herb-Synthesized Antiviral Nanoparticles. *Advance in Biological Research*, 3(1), 11-15. DOI: 10.26855/abr.2022.04.001

**Received:** March 23, 2022

**Accepted:** April 6, 2022

**Published:** April 20, 2022

**Corresponding author:** Yongqiang Jiang, State Key Laboratory of Pathogen and Biosecurity, Beijing Institute of Microbiology and Epidemiology, Beijing 100071, China.

**Email:** jiangyq@bmi.ac.cn

## Abstract

In 2016, Rasool et al. first noted that  $Ti_3C_2$  materials, with super antibacterial properties, makes two-dimensional nanomaterials as one of the most promising antibacterial nanomaterials into our focus. Gogotsi's study revealed that MXene materials have an ultrathin lamellar structure, and their antibacterial activity is remarkably better than that of graphene oxide materials. In this test,  $Ti_3C_2$ -Ag complexes were prepared by addition of silver-ammonia solution based on two-dimensional nano- $Ti_3C_2$  materials. Then antibacterial activity of the  $Ti_3C_2$ -Ag complexes against *Escherichia coli* (*E. coli*) and *Staphylococcus aureus* (*S. aureus*) was tested, antibacterial mechanism of the complexes was analyzed. This study found that the  $Ti_3C_2$ -Ag complexes could reach an antibacterial activity of 98.38% against *E. coli* and 99.08% against *S. aureus*. The antibacterial rate is positively correlated with silver content and action time. Their antibacterial mechanisms mainly included: (1) physical cutting of cell membranes by nanoscale sheets; (2) stimulating of oxidative stress response by silver nanoparticles, etc. The above results demonstrate that  $Ti_3C_2$ -Ag is a promising antibacterial material.

## Keywords

$Ti_3C_2$ -Ag Complexes, Preparation, Antibacterial, Mechanism

## 1. Introduction

New  $Ti_3C_2$  material and its synthesis method were first proposed by Professor Yury Gogotsi in 2011 [1], and the same research group reported ultra-strong antibacterial property of  $Ti_3C_2$  in 2016 [2], which is much stronger than that of graphene. The antibacterial property of  $Ti_3C_2$  has attracted many microbiologists; moreover, due to strong modification ability of rich groups on its surface, the surface modification of  $Ti_3C_2$  has become a new scientific research boom [3]. In 2020, Kaiyuan Zheng et al. developed a synergistic antibacterial agent via conjugation of ultra-small gold nanoclusters (AuNCs) on nanosheets. Ravi P. Pandey reported a silver nanoparticle-modified  $Ti_3C_2$  (Ag-MXene) film with more than 99% microbial inhibition rate against *Escherichia coli* (*E. coli*) [4]. Wei Wang et al. synthesized a novel copper oxide-anchored  $Ti_3C_2$  nanosheet with 97.4% antibacterial ability against *Staphylococcus aureus* (*S. aureus*) and 95.59% antibacterial property against *Pseudomonas aeruginosa* [5].

Two-dimensional nanomaterials represented by the  $Ti_3C_2$  complexes are triggering a global revolution in antibacterial technology, and continue to develop rapidly. In this paper,  $Ti_3C_2$ -Ag complexes were prepared, and their antibacterial ability was explored by studying the long-term antibacterial rate and antibacterial mechanism.

## 2. Materials and Methods

### 2.1 Reagents

Single-layer  $\text{Ti}_3\text{C}_2$  was purchased from Shandong Xiyuan New Material Technology Co., Ltd.; silver nitrate ( $\text{AgNO}_3$ ) solution was purchased from Sinopharm Chemical Reagent Co., Ltd.; and the test water was pure water ( $\text{ddH}_2\text{O}$ ).

### 2.2 Preparation and Purification of $\text{Ti}_3\text{C}_2$ -Ag Material

$\text{Ti}_3\text{C}_2$  was diluted and stirred for 30 min to prepare  $\text{Ti}_3\text{C}_2$  solution at 1 mg/mL concentration;  $\text{AgNO}_3$  solution was diluted to 0.01 mg/mL and sonicated for 10 min. According to the mass ratio of  $\text{AgNO}_3$  to  $\text{Ti}_3\text{C}_2$ , silver content was set to 12.5%, 25%, 37.5%, and 50%. The  $\text{AgNO}_3$  solution was dropped into the  $\text{Ti}_3\text{C}_2$  solution at a rate of 0.8 mL/min, stirred for 30 min, centrifuged at 10,000 r/min for 5 min, and washed three times to obtain four composites,  $\text{Ti}_3\text{C}_2$ -Ag12.5%,  $\text{Ti}_3\text{C}_2$ -Ag25%,  $\text{Ti}_3\text{C}_2$ -Ag37.5%, and  $\text{Ti}_3\text{C}_2$ -Ag50%, respectively.

### 2.3 Bacterial Information and Culture

Gram-negative bacteria: standard *E. coli* ATCC25922; Gram-positive bacteria: standard *S. aureus* USA300. The above strains were stored by the laboratory.

### 2.4 Study on Antibacterial Mechanism

In this long-acting antibacterial test (*E. coli* and *S. aureus*) with different concentrations of  $\text{Ti}_3\text{C}_2$ -Ag, four materials,  $\text{Ti}_3\text{C}_2$ -Ag12.5%,  $\text{Ti}_3\text{C}_2$ -Ag25%,  $\text{Ti}_3\text{C}_2$ -Ag37.5%, and  $\text{Ti}_3\text{C}_2$ -Ag50%, and a blank bacterial solution control were taken, with the concentrations of the materials set at 100 ug/mL and 200 ug/mL. They were mixed well with  $10^6$  CFU/mL *E. coli* or  $10^6$  CFU/mL *S. aureus*, placed for 2.5h, and diluted. Then the diluent was transferred to a constant temperature incubator for incubation at 37°C overnight to calculate bacteriostatic rate of the materials.

Calculation of antibacterial rate: antibacterial rate (100%) = (number of colonies in control group - number of colonies in experimental group)/number of colonies in control group \* 100%

Characterization of bacterial fluorescence by a confocal microscope: incubate *E. coli* in an incubator for 6 h, and then pipette 1 mL and centrifuge it at 10,000 r/min for 5 min. After that, aspirate the supernatant for protein leakage experiment ( $n = 3$ ). Re-suspend the bacteria at the bottom of the centrifuge tube with 0.5 mL PBS, stain them for 15 min with 2  $\mu\text{L}$  of Syto-9 and PI, respectively, and then use confocal laser scanning (Leica TCS SP8 SR, German) photography equipment: Canon camera (EOS 90D, Japan) for photographing.

Determination of bacterial protein leakage: take 200 ug/mL  $\text{Ti}_3\text{C}_2$ -Ag50% material and co-culture it with *E. coli* for 2.5 h, obtain the supernatant through high-speed centrifugation, extract the protein in it, and use a fluorospectrophotometer (Shanghai Lenguang Technology Co., Ltd., F96-pro) for testing.

Determination of bacterial reactive oxygen species (ROS) level: take 200 ug/mL  $\text{Ti}_3\text{C}_2$ -Ag50% material to interact with *E. coli* for 2.5 h. Then use a microplate reader (BIO-RAD, USA, model: iMark) in the fluorescence mode (excitation wavelength: 488 nm, emission wavelength: 525 nm) to determine the bacterial ROS level (The relative fluorescence intensity of the probe was represented as the ROS levels of the bacteria).

## 3. Results and Discussion

### 3.1 Analysis of Bacteriostasis

The results showed that  $\text{Ti}_3\text{C}_2$ -Ag12.5%,  $\text{Ti}_3\text{C}_2$ -Ag25%,  $\text{Ti}_3\text{C}_2$ -Ag37.5%, and  $\text{Ti}_3\text{C}_2$ -Ag50% had good antibacterial effect in the long-acting antibacterial test. At the concentration of 100 ug/mL, the bactericidal rates of the four materials against *E. coli* were 93.56%, 94.45%, 95.67%, 97.45%, respectively and the bactericidal rates against *S. aureus* were 94.23%, 94.56%, 95.45%, 96.32%, respectively. At the concentration of 200 ug/mL, the bactericidal rates of  $\text{Ti}_3\text{C}_2$ -Ag12.5%,  $\text{Ti}_3\text{C}_2$ -Ag25%,  $\text{Ti}_3\text{C}_2$ -Ag37.5%, and  $\text{Ti}_3\text{C}_2$ -Ag50% against *E. coli* were 97.67%, 97.45%, 96.45%, 98.08%, respectively; the bactericidal rates against *S. aureus* were 98.32%, 98.62%, 98.54%, 99.08%, respectively.

### 3.2 Characterization of Morphology Results

SEM in Figure 2a revealed that the bacteria (*E. coli*) in the control group had full morphology, smooth surface, and clear structure; the bacteria in the  $\text{Ti}_3\text{C}_2$ -Ag groups were wrapped by a large number of MXene sheets, having almost destroyed

cell membranes and cell walls and significantly shrunken morphology, and the cells lost their integrity. TEM in Figure 2b displayed that the bacteria in the control group had normal morphology, smooth cell surface, intact structure, full cytoplasm, and clear flagella and cell bodies (*E. coli*); the bacteria in the  $\text{Ti}_3\text{C}_2\text{-Ag}$  groups were wrapped by a large number of MXene sheets, showing a good adsorption capacity, the cell walls were destructed after inserted with some sheets, and the cytoplasm lost integrity after rupture and was significantly exposed.

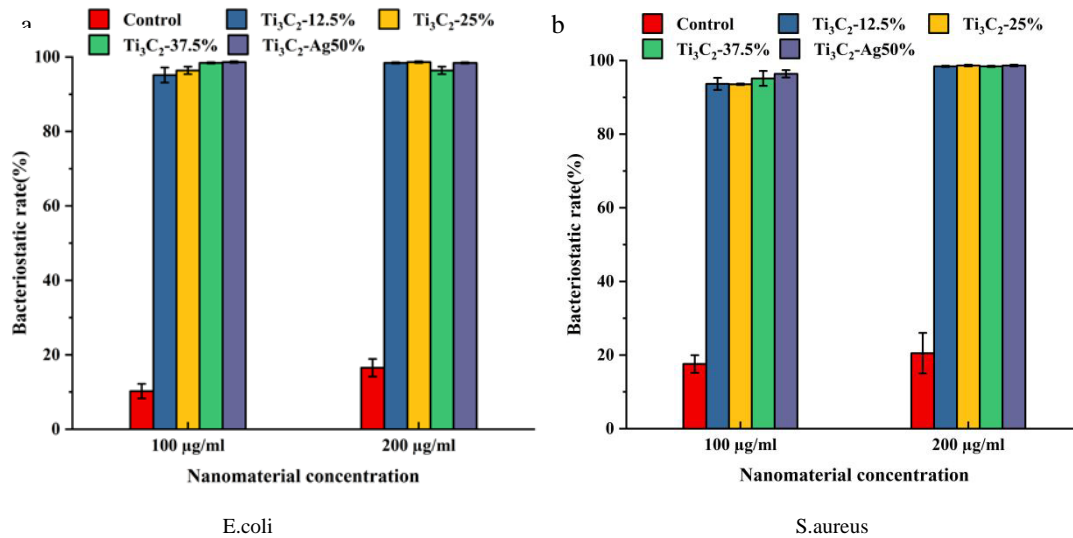


Figure 1. (a) Antibacterial rate of *E. coli* for  $\text{Ti}_3\text{C}_2\text{-Ag}$  complexes; (b) Antibacterial rate of *S. aureus* for  $\text{Ti}_3\text{C}_2\text{-Ag}$  complexes.

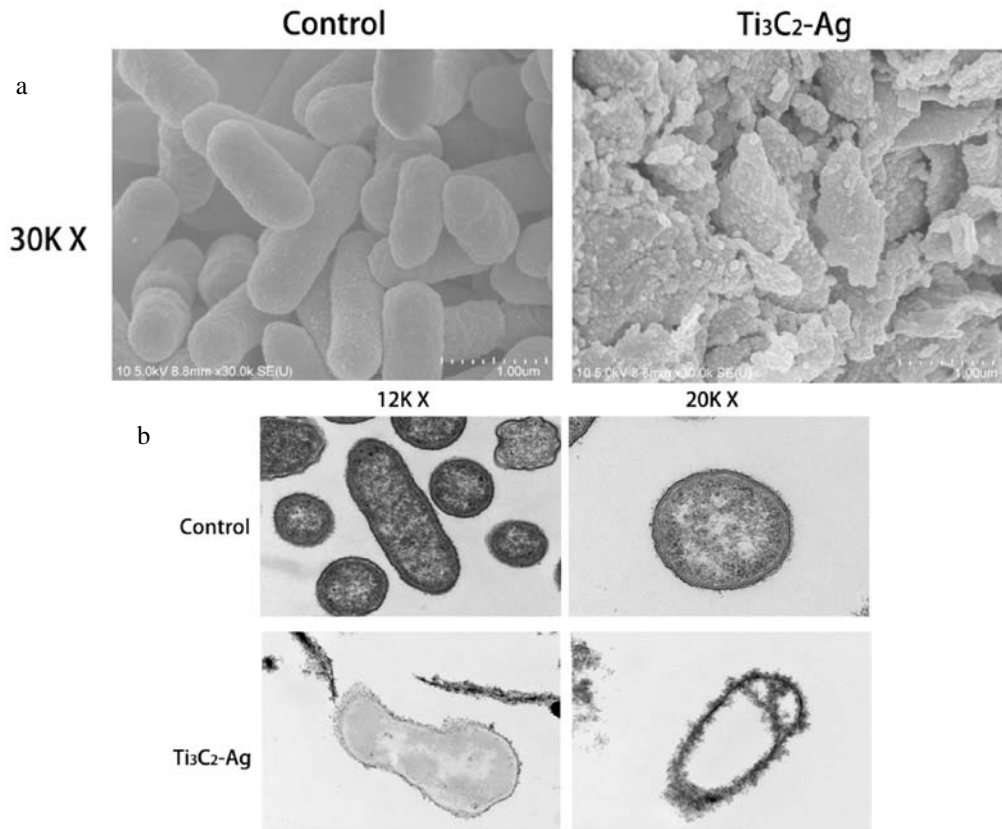


Figure 2. (a) SEM map of bacteria after interaction with  $\text{Ti}_3\text{C}_2\text{-Ag}$  complexes; (b) TEM map.

### 3.3 Fluorescence confocal map, protein leakage detection, intracellular ROS detection

The laser confocal test in Figure 3a showed overall antibacterial effect of the materials. After the  $\text{Ti}_3\text{C}_2\text{-Ag}$  complexes reacted with bacteria, the bacterial integrity was destroyed and most of the bacteria died. The above confirmed that the  $\text{Ti}_3\text{C}_2\text{-Ag}$  complexes had a strong antibacterial ability, and the composite nanomaterial could destroy the integrity of the cells, which was similar to the results of electron microscopy.

The leakage test of cytoplasmic components using protein as a representative index in Figure 3b revealed that only 0.011 mg/mL protein was found in the control group, while 0.308 mg/mL was found in the  $\text{Ti}_3\text{C}_2\text{-Ag}$  group, which was significantly higher and close to 30 times that in the former group. The results indicated that  $\text{Ti}_3\text{C}_2\text{-Ag}$  had considerable damage to bacteria and contributed to protein dissolution.

Bacterial ROS level in Figure 3c showed that  $\text{Ti}_3\text{C}_2\text{-Ag}$  caused severe damage to the bacterial structure and increased the bacterial ROS level. After the bacteria were exposed to the nanomaterial for 2 h, the bacterial ROS level in the test group (*E. coli* were treated with the nanomaterial at a concentration of 200  $\mu\text{g/mL}$ ) increased nearly 10-fold compared with that in the control group. This showed that after contact with the bacteria, the nanomaterial can not only destroy the cell membrane integrity through physical action, but also promote the occurrence of oxidative stress, thereby accelerating bacterial death and exerting antibacterial efficacy.

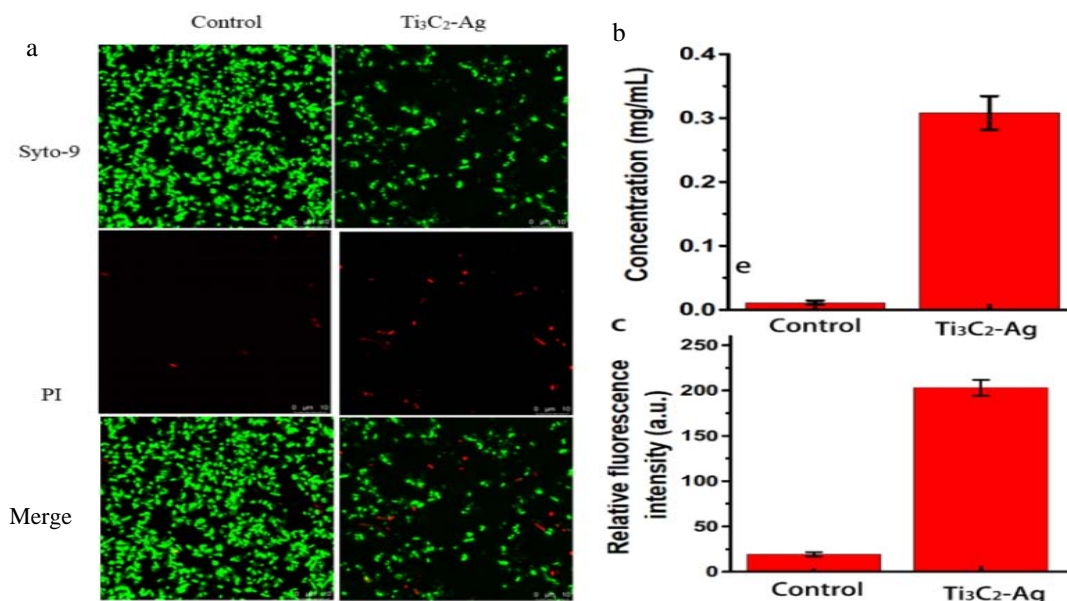


Figure 3. (a) Fluorescence confocal map; (b) Protein leakage after  $\text{Ti}_3\text{C}_2\text{-Ag}$  complexes and bacteria interaction; (c) Intracellular ROS level after  $\text{Ti}_3\text{C}_2\text{-Ag}$  complexes and bacteria interaction.

## 4. Discussion

By completing the antibacterial test of  $\text{Ti}_3\text{C}_2\text{-Ag}$  complexes, we obtained: (1) in the concentration range of 100  $\mu\text{g/mL}$  and 200  $\mu\text{g/mL}$ , the antibacterial rate gradually increased with the increase of concentration, but the increase was not very large; (2) in the case of the same concentration, the antibacterial rate gradually increased with the increase of AgNPs content, but the increase was not very large; (3) the bactericidal effect of  $\text{Ti}_3\text{C}_2\text{-Ag}$  materials on *S. aureus* was stronger than that on *E. coli*.

The antibacterial mechanism of  $\text{Ti}_3\text{C}_2\text{-Ag}$ : (1) The composite  $\text{Ti}_3\text{C}_2\text{-Ag}$  is able to cover bacterial surface in a faster and wider way since it is negatively charged on its surface and has a large specific surface area; (2) The composite  $\text{Ti}_3\text{C}_2\text{-Ag}$ , as a two-dimensional nanomaterial, has a relatively sharp nano-edge, which can physically destroy cell walls and induce bacterial death; (3) The composite  $\text{Ti}_3\text{C}_2\text{-Ag}$  is able to increase transmembrane permeability by surrounding bacterial biofilm, thus resulting in the leakage of substances in bacteria such as proteins; (4) The composite  $\text{Ti}_3\text{C}_2\text{-Ag}$  can induce oxidative stress in bacterial cells, especially, silver nanoparticles can promote the aggravation of oxidative stress in bacterial cells, thereby accelerating bacterial death.

Taken together, the two-dimensional nanocomposite  $\text{Ti}_3\text{C}_2\text{-Ag}$  has a good and relatively clear antibacterial property, which can serve as a new antibacterial material and a promising candidate in biomedical fields such as antibacterial new materials, antibacterial drugs and antibacterial cloth. Meanwhile there are still many problems to be solved for  $\text{Ti}_3\text{C}_2\text{-Ag}$  application in the biomedical fields, e.g., the biosafety of  $\text{Ti}_3\text{C}_2\text{-Ag}$ , which are also difficulties faced by two-dimensional nanomaterial researchers in the future.

## Acknowledgements

I would like to express my deepest gratitude to Dr. Shaolong Chen and Dr. Yongqiang Jiang for their suggestions comments and advice. I also thank my friends who give information, guidance, comments and suggestions.

## References

- [1] Naguib, Michael, Kurtoglu, Murat, Presser, Volker, Lu, Jun, Niu, Junjie, Heon, Min, et al. (2011). Two-dimensional nanocrystals produced by exfoliation of  $\text{Ti}_3\text{AlC}_2$ . *Advanced materials*, 23(37), 4248-4253.
- [2] Ghidui, Michael, Lukatskaya, Maria R, Zhao, Meng-Qiang, Gogotsi, Yury, and Barsoum, Michel W. (2014). Conductive two-dimensional titanium carbide 'clay' with high volumetric capacitance. *Nature*, 516(7529), 78-81.
- [3] Zhu, Jing, Ha, Enna, Zhao, Guoliang, Zhou, Yang, Huang, Deshun, Yue, Guozong, et al. (2017). Recent advance in MXenes: a promising 2D material for catalysis, sensor and chemical adsorption. *Coordination Chemistry Reviews*, 352, 306-327.
- [4] Shahzad, Faisal, Alhabeb, Mohamed, Hatter, Christine B, Anasori, Babak, Man Hong, Soon, Koo, Chong Min, et al. (2016). Electromagnetic interference shielding with 2D transition metal carbides (MXenes). *Science*, 353(6304), 1137-1140.
- [5] Ding, Li, Wei, Yanying, Li, Libo, Zhang, Tao, Wang, Haihui, Xue, Jian, et al. (2018). MXene molecular sieving membranes for highly efficient gas separation. *Nature communications*, 9(1), 1-7.
- [6] Kim, Seon Joon, Koh, Hyeong-Jun, Ren, Chang E, Kwon, Ohmin, Maleski, Kathleen, Cho, Soo-Yeon, et al. (2018). Metallic  $\text{Ti}_3\text{C}_2\text{T}_x$  MXene gas sensors with ultrahigh signal-to-noise ratio. *ACS nano*, 12(2), 986-993.